Normal or anomalous dispersion and gain in a resonant coherent medium

Hoonsoo Kang, Lingling Wen, and Yifu Zhu*
Department of Physics, Florida International University, Miami, Florida 33199, USA
(Received 21 January 2003; published 5 December 2003)

We show that in a four-level atomic system with electromagnetically induced transparency, a coherent pump field can induce light amplification without or with population inversion. As the pump field intensity increases, the atomic system evolves from normal dispersion and amplification without population inversion into anomalous dispersion and amplification with population inversion. We report an experiment on light amplification in cold rubidium atoms and present experimental measurements that agree with theoretical calculations based on the four-level model system.

DOI: 10.1103/PhysRevA.68.063806 PACS number(s): 42.50.Gy, 42.50.Hz, 32.80.−t

Dispersive and absorptive properties of an absorbing medium may be modified by coherence and interference induced by resonant laser fields, which lead to a variety of interesting phenomena for fundamental studies and practical applications. Much attention has been directed recently to coherent population trapping and electromagnetically induced transparency (EIT) [1,2], and their manifestation on the linear and nonlinear susceptibilities of optical media [3–8]. EIT manifested coherence and interference may lead to lasing without population inversion (LWI) [9–11] and selective enhancement or suppression of the higher-order nonlinear absorption and/or nonlinear light emission [12–21]. In particular, EIT has been used to enhance the nonlinear atomic dispersion [4,22] and to obtain light propagation with slow group velocities in an otherwise opaque medium [23–25]. In contrast to the slow group velocity, or subluminal light propagation in an EIT medium, superluminal light propagation occurs in optical media with anomalous dispersion [26–29]. Based on the anomalous dispersion induced in a double-peaked Raman gain medium, near distortion-free, gain-assisted superluminal light propagation has been observed recently [30].

Here, we show that EIT can be used to create either lasing without population inversion or lasing with inversion, with corresponding normal or anomalous dispersions that may be suitable for either gain-assisted subluminal or superluminal light propagations. Specifically, we show that in a four-level system with Λ-type EIT induced by a coupling laser and a weak probe laser, a pump laser coupled to a fourth level will induce amplification of the probe laser (see Fig. 1). With a weak pump laser, the probe amplification occurs without population inversion and the gain profile exhibits a single peak at the resonant probe transition. When the pump laser intensity increases, population inversion for the probe transition is created and the probe gain profile exhibits two peaks. Concurrently, the atomic dispersion experienced by the weak probe laser evolves from the normal shape into the anomalous shape, pointing to the possibility of the light propagation evolving from subluminal into superluminal. We present experimental measurements of the probe amplification in a four-level system realized with cold rubidium atoms, which demonstrates light amplification without or with population inversions and agrees with the four-level theoretical calculations.

Consider a four-level atomic system coupled by three laser fields as depicted in Fig. 1. Λ-type EIT is induced by a coupling laser driving the $|2\rangle \rightarrow |3\rangle$ transition and a probe laser driving the $|1\rangle \rightarrow |3\rangle$ transition. A pump laser driving the $|1\rangle \rightarrow |4\rangle$ transition controls the population inversion between the states $|3\rangle$ and $|1\rangle$, which determines the probe absorption/gain. For later discussions g, Ω_c and Ω' are defined as half Rabi frequencies for the probe transition $|1\rangle \rightarrow |3\rangle$, the coupling transition $|2\rangle \rightarrow |3\rangle$, and the pump transition $|1\rangle \rightarrow |4\rangle$, respectively. $\Delta_c = \omega_c - \omega_{32}$, $\Delta' = \omega' - \omega_{41}$, and $\Delta = \omega_p - \omega_{31}$ denote the frequency detuning of the coupling laser, the pump laser and the probe laser, respectively. The density matrix equation for the four-level systems under the dipole interaction and the rotating-wave approximation is given by

$$\frac{d\rho_{11}}{dt} = \gamma_{31}\rho_{33} + \gamma_{41}\rho_{44} + ig(\rho_{31} - \rho_{13}) + i\Omega'(\rho_{41} - \rho_{14}), \tag{1a}$$

$$\frac{d\rho_{22}}{dt} = \gamma_{32}\rho_{33} + \gamma_{42}\rho_{44} + i\Omega_c(\rho_{32} - \rho_{23}), \tag{1b}$$

$$\frac{d\rho_{33}}{dt} = -(\gamma_{32} + \gamma_{31})\rho_{33} + ig(\rho_{13} - \rho_{31}) + i\Omega_c(\rho_{23} - \rho_{32}), \tag{1c}$$

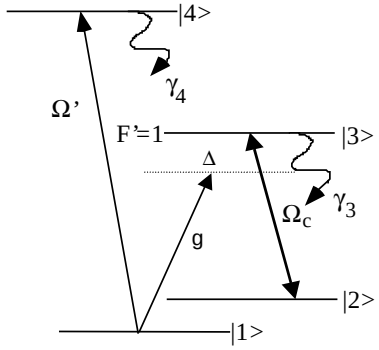

FIG. 1. Four-level Λ-type atomic system and laser coupling scheme. γ_3 and γ_4 are the spontaneous decay rates.

*Email address: yifuzhu@fiu.edu

 ©2003 The American Physical Society

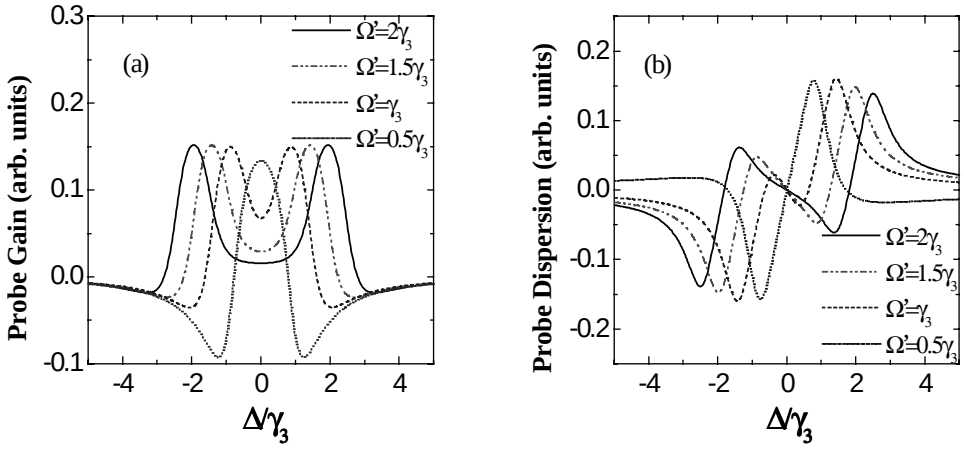

FIG. 2. (a) Calculated probe gain $[\mathrm{Im}(\rho_{13})]$ and (b) calculated probe dispersion $[\mathrm{Re}(\rho_{13})]$ versus the probe detuning Δ for the four-level EIT system. The parameters are $\Omega_c=0.5\gamma_3$, $g=0.01\gamma_3$, $\gamma_4=1.2\gamma_3$, and $\gamma_{21}=0.001\gamma_3$. Note that as Ω' increases, the gain profile evolves from the single-peaked line profile (without inversion) into the double peaked line profile (with population inversion). The probe dispersion evolves correspondingly from the normal line shape into the anomalous line shape.

$$\frac{d\rho_{44}}{dt}=-(\gamma_{42}+\gamma_{41})\rho_{44}+i\Omega'(\rho_{14}-\rho_{41}), \tag{1d}$$

$$\frac{d\rho_{12}}{dt}=-[\gamma_{21}+i(\Delta-\Delta_c)]\rho_{12}-i\Omega_c\rho_{13}+i\Omega'\rho_{42}+ig\rho_{32}, \tag{1e}$$

$$\frac{d\rho_{13}}{dt}=-[(\gamma_{31}+\gamma_{32}+\gamma_{21})/2+i\Delta]\rho_{13}+ig(\rho_{33}-\rho_{11}) -i\Omega_c\rho_{12}+i\Omega'\rho_{43}, \tag{1f}$$

$$\frac{d\rho_{14}}{dt}=-[(\gamma_{21}+\gamma_{41}+\gamma_{42})/2+i\Delta']\rho_{14}+i\Omega'(\rho_{44}-\rho_{11}) +ig\rho_{34}, \tag{1g}$$

$$\frac{d\rho_{23}}{dt}=-[(\gamma_{31}+\gamma_{32}+\gamma_{21})/2+i\Delta_c]\rho_{23}+i\Omega_c(\rho_{33}-\rho_{22}) -ig\rho_{21}, \tag{1h}$$

$$\frac{d\rho_{24}}{dt}=-[(\gamma_{41}+\gamma_{42}+\gamma_{21})/2+i(\Delta_c+\Delta'-\Delta)]\rho_{24}-i\Omega'\rho_{21} +i\Omega_c\rho_{34}, \tag{1i}$$

$$\frac{d\rho_{34}}{dt}=-[(\gamma_{31}+\gamma_{32}+\gamma_{41}+\gamma_{42})/2+i(\Delta'-\Delta)]\rho_{34}+ig\rho_{14} +i\Omega_c\rho_{24}-i\Omega'\rho_{31}, \tag{1j}$$

where $\gamma_3=\gamma_{31}+\gamma_{32}$ and $\gamma_4=\gamma_{41}+\gamma_{42}$ are the decay rates for the states $|3\rangle$ and $|4\rangle$, respectively. γ_{21} is the dephasing rate between the states $|1\rangle$ and $|2\rangle$. We note that the similar four-level *N*-type system has been analyzed recently [31] and the theoretical model may well be adapted to the four-level system studied here. The emphasis of Ref. [31] is in the context of electromagnetically induced absorption, in which spontaneous coherence transfer is responsible for the occurrence of subnatural resonance. Such spontaneous coherence transfer may be viewed as due to the decay branching ratio in a partially open system and an additional coupling term is introduced between the density matrix elements ρ_{34} and ρ_{12} [31]. In contrast, we consider the four-level system in Fig. 1 closed such that $\rho_{11}+\rho_{22}+\rho_{33}+\rho_{44}=1$, and do not include the spontaneous coherence transfer in Eq. (1). Furthermore, for the closed EIT system, the adiabatic steady state is reached when $t\gg 1/\gamma_3$ and $1/\gamma_4$ ($\gamma_{12}\ll\gamma_3$ and γ_4) while for the open system exhibiting electromagnetically induced absorption, the time to reach the steady state is considerably slower [32].

We are interested in the case of resonant excitations, i.e., $\Delta_c=\Delta'=0$, in which the EIT effect is the most prominent and the coherent pumping is the most efficient. We have

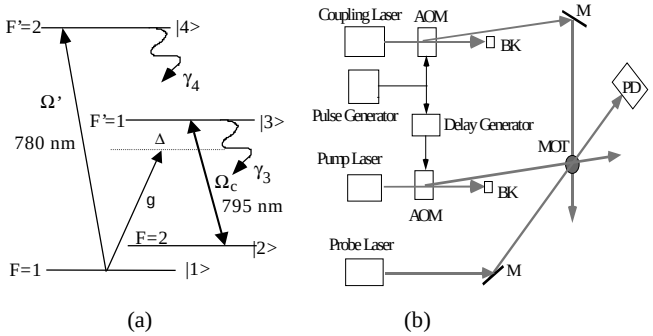

FIG. 3. (a) Energy levels and laser coupling scheme for ^{87}Rb atoms. (b) Schematic diagram of the experimental set up. AOM: acousto-optic modulator; M: mirror; BK: beam blocker; PD: photo detector. The experiment is running at a repetition rate of 20 Hz. For each period, the cooling and trapping lasts for 199 ms, during which the coupling laser and the pump laser are off; the probe transmission measurement runs for 1 ms, during which the coupling laser and the pump laser are turned on, and the probe is scanned across the $5S_{1/2}$, $F=1\rightarrow 5P_{1/2}$, $F=1$ transition (the trap laser and the repump laser are turned off).

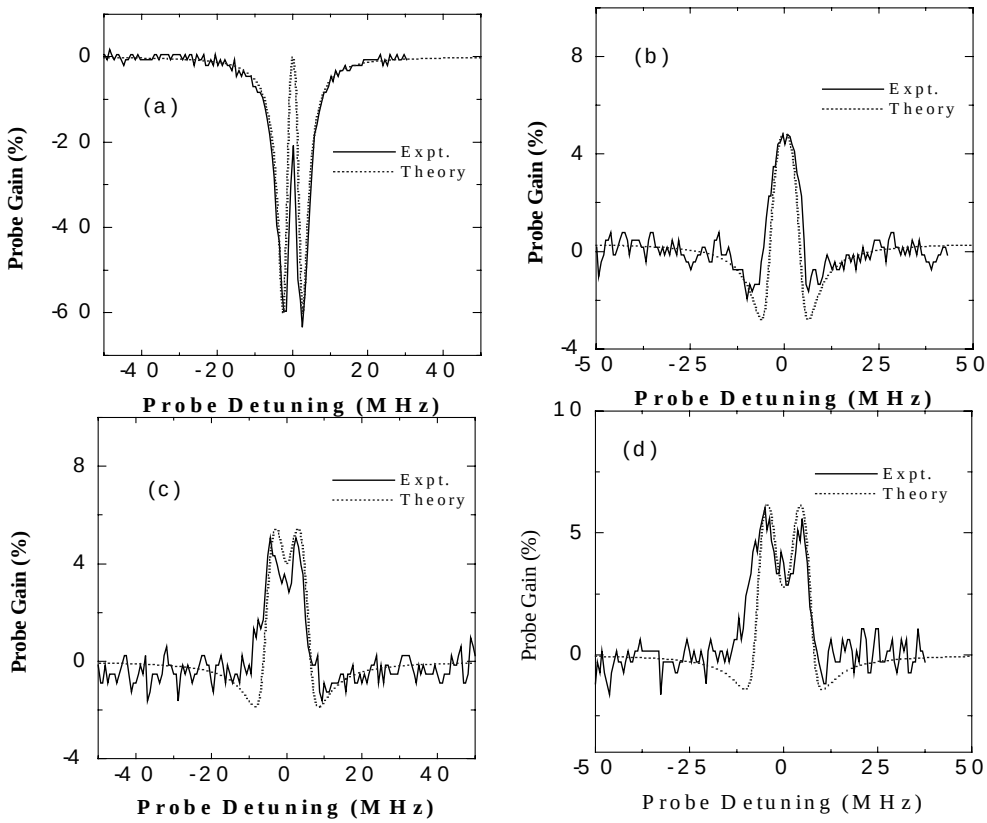

FIG. 4. Measured probe transmission spectra versus the probe frequency detuning Δ. (a) The EIT spectrum without the pump laser. (b) The probe gain spectrum with the pump laser intensity at ~ 4 mW/cm^2. (c) The probe gain spectrum with the pump laser intensity at ~ 9 mW/cm^2. (d) The probe gain spectrum with the pump laser intensity at ~ 16 mW/cm^2. The solid lines are the experimental data and the dotted lines are the theoretical calculations based on the four-level Rb system of Fig. 2(a). The fitting parameters are $2\Omega_c = \gamma_3$, $g = 0.01\gamma_3$, and $\gamma_{21} = 0.001\gamma_3$ ($\gamma_3/2\pi = 5.3$ MHz and $\gamma_4/2\pi = 5.9$ MHz). $2\Omega' = \gamma_3$, $1.5\gamma_3$, and $2\gamma_3$ in (b), (c), and (d), respectively.

numerically solved Eq. (1) in the steady state under a variety of conditions. The calculations show that for fixed Ω_c and g values, as the pump Rabi frequency Ω' increases from zero up, the absorptive response of the probe laser in the four-level system evolves from EIT [$\mathrm{Im}(\rho_{13}) = 0$ at $\Delta = 0$] into amplification without inversion [$\mathrm{Im}(\rho_{13}) > 0$ at $\Delta = 0$ and $\rho_{11} > \rho_{33}$]. The probe gain exhibits a spectral line profile with the peak gain at $\Delta = 0$ manifested by the constructive interference [11,33–35]. The corresponding dispersive response of the probe laser shows the normal positive slope near $\Delta = 0$, which leads to a slow group velocity. Further increase of the pump Ω' results in the population inversion $\rho_{33} > \rho_{11}$ and the probe gain spectrum exhibit double peaks located at $\Delta \approx \pm\Omega'$, which corresponds to the energy separation of the two dressed states $[(1/\sqrt{2})(|4\rangle + |1\rangle)]$ and $[(1/\sqrt{2})(|4\rangle - |1\rangle)]$ created by the coherent pump field. The corresponding dispersion becomes anomalous and exhibits a negative slope near $\Delta = 0$, which is similar to Ref. [30] and leads to superluminal light propagation. Figure 2(a) plots the absorptive/gain response of the weak probe laser and Fig. 2(b) plots the dispersive response of the probe laser versus the probe frequency detuning Δ for several values of the pump Rabi frequency Ω'. The calculations show that with a moderate coupling laser and a weak probe laser ($\Omega_c = 0.5\gamma_3$ and $g = 0.01\gamma_3$), when $\Omega' < 0.7\gamma_3$, there is no population inversion ($\rho_{11} > \rho_{33}$), the system exhibits amplification without inversion and normal dispersion; when $\Omega' > 0.7\gamma_3$, population inversion is created ($\rho_{33} > \rho_{11}$), the probe gain exhibits the double peak profile and the atomic dispersion is anomalous.

The laser coupling scheme for ^{87}Rb atoms used in our experiment is depicted in Fig. 3(a). EIT in the Rb atomic system is induced by a coupling laser driving the D_1 $5S_{1/2}$, $F = 2 \rightarrow 5P_{1/2}$, $F' = 1$ transition and a probe laser driving the D_1 $5S_{1/2}$, $F = 1 \rightarrow 5P_{1/2}$, $F' = 1$ transition [33]. Probe amplification is induced by a pump laser driving the D_2 $5S_{1/2}$, $F = 1 \rightarrow 5P_{3/2}$, $F' = 2$ transition. The probe laser and the pump laser are linearly polarized parallel with each other, which is perpendicular to the linearly polarized coupling laser. The induced transitions among the magnetic sublevels by the three lasers can be grouped together according to the selection rules and form a manifold of Λ-type four-level systems. To a good approximation, the coupled Rb system can be viewed as equivalent to a generic Λ-type four-level system depicted in Fig. 3(a). The validity of such a simplification has been supported by several previous EIT-type studies in alkaline atoms [11,19,33,34]. Our experiments are done in a vapor cell magneto-optical trap (MOT) produced in the center of a ten-ports, 4-1/2 in. diameter, stainless-steel vacuum chamber pumped down to a pressure $\sim 10^{-9}$ torr. The rubidium vapor pressure of $\sim 10^{-8}$ torr is maintained with three rubidium getters connected in a series and placed

close to the center of the vacuum chamber. A diode laser-tapered amplifier system (TA-100, Tuioptics) with an output power of ~300 mW is used as the cooling and trapping laser that supplies six σ^+ and σ^- polarized beams in three perpendicular spatial directions and its frequency is locked to ~15 MHz below the D_2 $F=2\rightarrow F'=3$ transition. An extended-cavity diode laser with an output power of ~20 mW is used as the repump laser and its frequency is locked on the D_2 $F=1\rightarrow F'=2$ transition. The diameter of the trapping laser beams and the repumping laser beam is ~2.5 cm. The trapped ^{87}Rb atom cloud is ~3 mm in diameter and contains $\sim 10^9$ atoms. A simplified experimental scheme is depicted in Fig. 2(b). The probe laser is provided by a third extended-cavity diode laser with a beam diameter ~1 mm and its power attenuated to ~10 μW. The coupling field is provided by a fourth extended-cavity diode laser with a beam diameter ~5 mm and output power ~20 mW. A fifth extended-cavity diode laser with a beam diameter ~5 mm is used as the pump laser. The laser intensities are varied by neutral density filters. The linewidth of the extended-cavity diode lasers is ~1 MHz. The probe laser, the coupling laser, and the pump laser are overlapped with the trapped Rb cloud and the transmitted light of the probe laser is recorded by a photodiode detector. The probe laser, the coupling laser, and the signal laser are overlapped with the trapped Rb cloud. The probe laser and the signal laser propagating at an angle of ~4° relative to each other have a spatial angle of ~45° relative to the propagating direction of the coupling laser. The effects of nonlinear wave mixing are frequently observed in the vapor cell experiments where collinear-propagating lasers are employed. The noncollinear excitation scheme used in our experiment should minimize the effects of the nonlinear wave mixing (such as four-wave mixing processes) on the response of the probe laser since it usually does not meet the phase matching condition.

The experiment is run in a sequential mode with a repetition rate of 5 Hz. All lasers except the probe laser are turned on and off by acousto-optic modulators (AOM) according to the time sequence described below. For each period of 200 ms, ~199 ms is used for cooling and trapping of the Rb atoms during which the trap laser and the repump laser are turned on by two separate AOMs while the coupling laser and the pump laser are off. The weak, continuous probe laser does not disturb the MOT. The time for the measurements of the probe transmission lasts ~1 ms during which the trap laser and the repump laser are turned off, and the coupling laser and the pump laser (with their frequencies locked on the D_1 $F=2\rightarrow F'=1$ transition and D_2 $F=1\rightarrow F'=2$ transition, respectively) are turned on by two additional AOMs. After a 10 μs delay, the probe laser frequency is scanned across the D_1 $F=1\rightarrow F'=1$ transition in ~0.3 ms and the probe transmission is recorded by a digital oscilloscope (Tektronix TDS460). Since the laser pulse durations are much greater than the atomic decay times $1/\gamma_3$ (30 ns) and $1/\gamma_4$ (27 ns) the measurements are carried out essentially in the adiabatic steady-state regime.

Figure 4 shows the measured transmission spectrum of the probe laser versus the probe frequency detuning Δ. The solid lines are the experimental measurements while the dotted lines are the theoretical calculations based on the four-level EIT model. Within the experimental uncertainty, the experimental data agree with the theoretical calculations. Figure 4(a) is the usual EIT spectrum (without the pump laser) with the measured Rabi frequency $\Omega_c \approx 5$ MHz. Figure 4(b) presents the probe gain spectrum of amplification without inversion for the pump laser intensity ~4 mW/cm^2. Figures 4(c) and 4(d) present the probe gain spectra with the pump laser intensities ~9 and 16 mW/cm^2, respectively, showing the double-peak line profile, which is similar to the probe amplification spectra observed in a *V*-type system [34]. Our calculations indicate that when the probe gain evolves from a single-peak spectrum into a double-peak spectrum, the population distribution evolves correspondingly from noninversion, $\rho_{33}<\rho_{11}$, into population inversion, $\rho_{33}>\rho_{11}$.

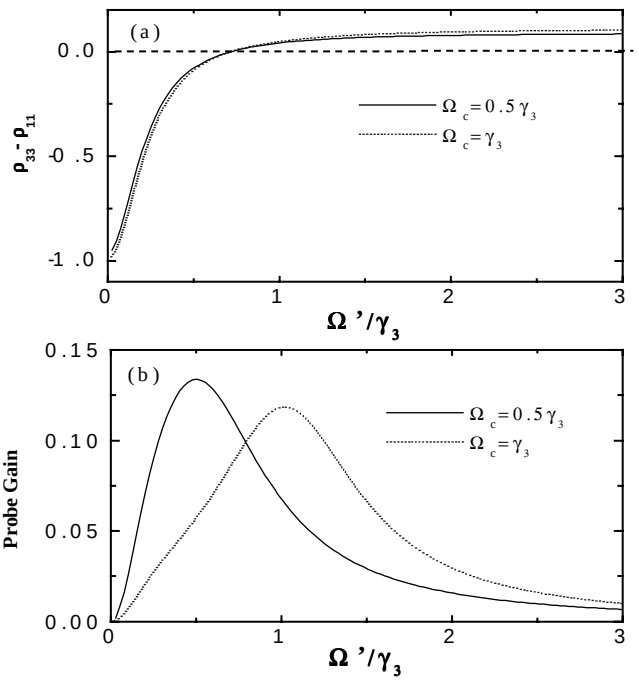

FIG. 5. (a) Calculated population difference, $\rho_{33}-\rho_{11}$ and (b) calculated probe gain [Im(ρ_{13})] at $\Delta=0$ versus the pump Ω'. The parameters are $g=0.01\gamma_3$, $\gamma_{21}=0.001\gamma_3$, and $\gamma_4=1.2\gamma_3$. The probe gain [Im(ρ_{13})] at $\Delta=0$, which is contributed by the constructive interference, approaches a maximum value at a moderate Ω' value, then decreases monotonically while the population inversion approaches the saturation value.

In order to show explicitly the dependence of the probe amplification with and without the population inversion on the pump laser intensity, we plot in Fig. 5(a) the calculated population inversion and Fig. 5(b) the probe gain [Im(ρ_{13})] at the probe resonance ($\Delta=0$) versus the pump Rabi frequency Ω' for two Ω_c values. The probe gain at $\Delta=0$ is mainly manifested by constructive interference [11,34,35] and as the pump laser intensity increases, the energy splitting of the two dressed states created by the pump laser $2\Omega'$ becomes large, which results in a large detuning for the LWI gain manifested by the constructive interference and leads to a decreasing LWI gain versus Ω' as shown in Fig. 4(b).

In conclusion, we have shown theoretically that EIT in a Λ-type system may be used to create either lasing without population inversion or lasing with inversion by applying a coherent pump field coupled to a fourth level. The coherent pump can be used to control the population distribution in the four-level system, realizing amplification without inversion with a normal dispersion or double peaked gain with inversion and anomalous dispersion. Therefore the system may be suitable for further studies of either gain-assisted subluminal or superluminal light propagation. We have presented experimental measurements of the probe amplification, which agree with the calculated probe amplification without inversion or with population inversion based on the four-level Rb system.

This work is supported by the National Science Foundation and the Office of Naval Research.

[1] E. Arimondo, in *Progress in Optics*, edited by E. Wolf (Elsevier Science, Amsterdam, 1996), p. 257–354.
[2] S. E. Harris, Phys. Today **50**, 36 (1997).
[3] S. E. Harris, Phys. Rev. Lett. **62**, 1033 (1989).
[4] M. O. Scully and M. Fleischhauer, Phys. Rev. Lett. **69**, 1360 (1992).
[5] G. S. Agarwal and S. P. Tewari, Phys. Rev. Lett. **70**, 1417 (1993).
[6] G. S. Agarwal and W. Harshawardhan, Phys. Rev. Lett. **77**, 1039 (1996).
[7] H. Schmidt and A. Imamoglu, Opt. Lett. **21**, 1936 (1996).
[8] M. Fleischhauer, C. H. Keitel, M. O. Scully, C. Su, S. T. Ulrich, and S. Y. Zhu, Phys. Rev. A **46**, 1468 (1992).
[9] O. Kocharovskaya, Phys. Rep. **219**, 175 (1992).
[10] M. O. Scully, Phys. Rep. **219**, 191 (1992).
[11] G. G. Padmabandu, G. R. Welch, I. N. Shubin, E. S. Fry, D. E. Nikonov, M. D. Lukin, and M. O. Scully, Phys. Rev. Lett. **76**, 2053 (1996).
[12] K. Hakuta, L. Marmet, and B. P. Stoicheff, Phys. Rev. Lett. **66**, 596 (1991).
[13] G. Z. Zhang, K. Hakuta, and B. P. Stoicheff, Phys. Rev. Lett. **71**, 3099 (1993).
[14] M. Jain, A. J. Merriam, A. Kasapi, G. Y. Yin, and S. E. Harris, Phys. Rev. Lett. **75**, 4385 (1995).
[15] M. D. Lukin, P. R. Hemmer, M. Loffler, and M. O. Scully, Phys. Rev. Lett. **81**, 2675 (1998).
[16] Y. Li and M. Xiao, Opt. Lett. **21**, 1064 (1996).
[17] H. Wang, D. Goorskey, and M. Xiao, Phys. Rev. Lett. **87**, 073601 (2001).
[18] S. E. Harris and Y. Yamamoto, Phys. Rev. Lett. **81**, 3611 (1998).
[19] M. Yan, E. Rickey, and Y. Zhu, Opt. Lett. **26**, 548 (2001).
[20] M. Yan, E. Rickey, and Y. Zhu, Phys. Rev. A **64**, 043807 (2001).
[21] A. S. Zibrov, M. D. Lukin, L. Hollberg, and M. O. Scully, Phys. Rev. A **65**, 051 801(R) (2002).
[22] A. S. Zibrov, M. D. Lukin, L. Hollberg, D. E. Nikonov, M. O. Scully, H. G. Robinson, and V. L. Velichansky, Phys. Rev. Lett. **76**, 3935 (1996).
[23] L. V. Hau, S. E. Harris, Z. Dutton, and C. H. Behroozi, Nature (London) **397**, 594 (1997).
[24] M. M. Kash, V. A. Sautenkov, A. S. Zibrov, L. Hollberg, G. R. Welch, M. D. Lukin, Y. Rostovtsev, E. S. Fry, and M. O. Scully, Phys. Rev. Lett. **82**, 5229 (1999).
[25] D. Budker, D. F. Kimball, S. M. Rochester, and V. V. Yashchuk, Phys. Rev. Lett. **83**, 1767 (1999).
[26] R. Y. Chiao, Phys. Rev. A **48**, R34 (1993).
[27] A. M. Steinberg and R. Y. Chiao, Phys. Rev. A **49**, 2071 (1994).
[28] A. M. Akulshin, S. Barreiro, and A. Lezama, Phys. Rev. Lett. **83**, 4277 (1999).
[29] R. W. Boyd and D. J. Gauthier, Prog. Opt. **43**, 497 (2002).
[30] L. J. Wang, A. Huzmich, and A. Dogariu, Nature (London) **406**, 277 (2000).
[31] A. V. Taichenachev, A. M. Tumaikin, and V. I. Yudin, Phys. Rev. A **61**, 011 802 (1999).
[32] P. Valente, H. Failache, and A. Lezama, Phys. Rev. A **67**, 013 806 (2003).
[33] M. Yan, E. Rickey, and Y. Zhu, J. Opt. Soc. Am. B **18**, 1057 (2001).
[34] J. Kitching and L. Hollberg, Phys. Rev. A **59**, 4685 (1999).
[35] Y. Zhu, Phys. Rev. A **45**, R6149 (1992).